This is the preprint version of the article that appeared in final form in **Journal of Nuclear Materials** 549 : (2021) // Article ID 152907, which has been published in final form at https://doi.org/10.1016/j.jnucmat.2021.152907.

Infrared emissivity of reduced-activation Eurofer 97 for fusion reactor applications

T. Echániz[a,*], I. González de Arrieta[b,c], A. Gil-Muñoz[b], J. Fernández-Pereda[b], R. Fuente[a], M. Klimenkov[d], G.A. López[b]

[a] *Applied Mathematics, University of the Basque Country UPV/EHU, E-48013 Bilbao, Spain*
[b] *Physics Department, University of the Basque Country UPV/EHU, E-48940 Leioa, Spain*
[c] *CNRS, CEMHTI UPR3079, Univ. Orléans, F-45071 Orléans, France*
[d] *Karlsruhe Institute of Technology (KIT), Institute for Applied Materials-Applied Materials Physics, D-76021 Karlsruhe, Germany*

Abstract

The spectral directional emissivity of Eurofer 97 is reported between 423 and 873 K for two surface states. Total hemispherical data has been calculated by numerical integration of the measured data and compared to the theoretical predictions based on electrical resistivity data. It is shown that the significant differences in the latter property between Eurofer 97 and similar steels (Grade 91, F82H) do not translate into notably dissimilar thermal radiative properties. However, the surface state can be shown to greatly influence the results beyond any intrinsic effects. Finally, the reported values for a polished surface are shown to be comparable to data for Grade 91 steel and lower than the usually assumed ones in thermal budget modelling of the DEMO tokamak and other nuclear applications of this alloy.

Keywords: Eurofer 97, infrared emissivity, low-activation materials, heat transfer, ferritic-martensitic steels

1. Introduction

Reduced Activation Ferritic/Martensitic (RAFM) steels are one of the very few types of materials compatible with the demands of high-temperature mechanical strength and low activation that are required for structural materials in nuclear fusion reactors [1]. The 9Cr-1W-V-Ta composition known as Eurofer

*Corresponding author.
Email address: telmo.echaniz@ehu.eus (T. Echániz)

97 is one of the most widely studied candidates for this application. Its main limitation is the upper temperature limit of 823 K, which can be raised to 923 K by oxide-dispersion-strengthening [2].

Due to the stringent thermo-mechanical demands for nuclear fusion reactor designs, thermophysical characterizations of candidate structural materials are of crucial significance. In the case of Eurofer 97, several of its thermophysical properties have been characterized and compared to those of the Japanese alternative F82H (8Cr-2W-V-Ta) [3], as well as their mechanical properties at high temperatures [1]. These properties can be used in thermal simulations of heat transfer inside the vessel [4–7]. However, there is a notable absence of emissivity measurements in these characterizations. This defficiency contrasts with the important role of this parameter in temperature measurements and heat transfer of reduced-activation materials for neutronics research and nuclear fusion applications [8–11].

Infrared emissivity data are generally scarce in the thermophysical literature, often with contradictory results being reported. In the field of nuclear-grade steels, some data can be found [12–18]. However, there is currently no data available on the emissivity of Eurofer 97, despite several works reporting on values of this property for relatively similar 9Cr-1Mo ferritic steels [12–15]. As is the case with many alloys, infrared emissivity data can be inferred from published electrical resistivity measurements, but the accuracy of this procedure is difficult to know *a priori* [19]. Therefore, measurements of their thermal radiative properties need to be performed to provide accurate data, especially when differences in surface states of the alloys are expected. In the case of this material, emissivity values around 0.25 have been assumed in heat transfer simulations of the DEMO tokamak [4–6], as well as for determining temperatures in experiments concerning Eurofer 97 [20]. Even higher values have been assumed in other works, from 0.3 to $0.5 - 0.6$ [8–10]. In this regard, this work aims to provide reliable data for the thermal radiative properties of this nuclear alloy, continuing the path previously started for samples of the V-4Cr-4Ti family [21].

2. Materials and methods

The sample, as supplied by the Karlsruhe Institute of Technology (EUROFER 97-2, batch 993391 [22]), was a 6-mm-thick plate processed by hot rolling. The sample was austenitized at 1233 K with oil quenching followed by tempering at 1023 K. Its chemical composition in wt% is 8.83 Cr−1.08 W−0.2 V−0.12 Ta−0.1 C−0.02 N. It was characterized with two surface states: as rolled, and polished with SiC grit paper (last number: 4000). The roughness values were measured in two perpendicular directions with a mechanical profilometer before and after the emissivity measurements. A microstructural characterization was performed using X-ray diffraction and transmission electron microscopy (TEM). X-ray diffraction measurements were done with Cu K_α radiation in the Bragg-Brentano geometry. TEM measurements were performed at Karlsruhe Institute of Technology using a FEI Tecnai 20 FEG microscope with an accelerating voltage of 200 kV, scanning unit for performing scanning TEM (STEM) with high angle annular dark field (HAADF) detector, Gatan Image Filter (GIF) and an EDX detector for elemental analysis.

The emissivity measurements were made with the high-accuracy HAIRL emissometer of the University of the Basque Country (UPV/EHU), a device which can measure spectral emissivity values at high temperatures in vacuum [23]. The sample temperature was measured by two type K thermocouples spot-welded onto the surface of the material. The combined standard uncertainty of the spectral emissivity measurements in metals increases with wavelength and decreases with temperature. The total emissivities were calculated using the following equations:

$$\varepsilon_T(\theta, T) = \frac{\int_0^\infty \varepsilon(\lambda, \theta, T) L_{bb}(\lambda, T) d\lambda}{\int_0^\infty L_{bb}(\lambda, T) d\lambda}, \tag{1}$$

$$\varepsilon_H(T) = \int_0^{\pi/2} \varepsilon_T(\theta, T) \sin(2\theta) d\theta, \tag{2}$$

where θ is the polar angle, L_{bb} is the radiance of a blackbody as given by Planck's law, ε_T stands for the total directional emissivity (total normal, in the special case of $\theta = 0$), and ε_H stands for the total hemispherical emissivity. A Monte Carlo random-number sampling procedure has been used to propagate the uncertainties of these quantities, where the inputs in the integral calculations are

modelled as probability distributions, based on their statistical properties [24]. Furthermore, an extrapolation procedure was used to introduce unbiased estimations of the amount of radiation outside the measured spectral range, based on the well-known spectrally monotonic emissivities of metals. The contribution of these off-range integrations in Eq. 1 remained a small part of the total weight for all temperatures under study [23].

The sample was measured in Ar (99.999%) to improve thermal contact and stability. A protective Zr foil was introduced in the setup to reduce the probability of high-temperature oxidation by residual oxygen. Measurements were performed up to 873 K due to the potential degradation of the sample at higher temperatures, as the 873–973 K window induces the $M_{23}C_6$ precipitate growth [25, 26]. X-ray diffraction and scanning electron microscopy (SEM) were used to characterize the samples after the emissivity measurements, without any signs of significant oxygen uptake or degradation.

3. Results and discussion

An X-ray diffractogram is shown in Fig. 1. The three peaks correspond to the BCC (Fe) solid solution with a lattice parameter $a = 2.866$ Å, which compares satisfactorily to the value $a = 2.862$ Å expected for a steel with Fe−9.5at%Cr composition [3]. Fig. 2a shows the typical lath martensite structure of this alloy. Fig. 2b illustrate analytical TEM study of the chemical replica of Eurofer 97. Different precipitates can be discerned by color: Cr-rich $M_{23}C_6$ precipitates are shown in green, VN in blue, and TaC in red. While the latter two consist of small grains, the size of individual $M_{23}C_6$ precipitates can achieve values up to 250 nm. These results correlate well to those in the literature [25, 26].

Two surface states have been studied: the as-rolled state and a polished one. The surface parameters are shown in Table 1, where R_a is the average roughness, R_q the root-mean-square roughness, R_z the average maximum height, and RSm the mean spacing between profile elements. No significant differences were observed between roughness values measured before and after the emissivity measurements. It is interesting to note that the value characterizing the horizontal spread of the profile, RSm is larger for the as-rolled state than for the polished one. This suggests that, despite this surface having prominent peaks

Table 1: Roughness parameters of the sample surface (in μm).

State	R_a	R_q	R_z	RSm
As rolled	5.82	7.22	30.9	183
Polished	0.06	0.09	0.38	69

and valleys, the average correlation length of its roughness features is larger.

Normal spectral emissivity data for the as-rolled and polished surface states are shown in Fig. 3. The usual tendencies for metallic materials can be appreciated, with emissivities that increase with temperature and decrease with wavelength [19]. As expected, the as-rolled texture features significantly larger emissivity values than the polished one, consistent with its larger surface roughness, but still retains the general metallic emissivity trends. The presence of small spectral features at 4.2, $6-7$ and 14.5 μm correspond to the contamination by residual atmospheric gases in the blackbody optical path. The reproducibility of the data was checked by performing successive heating cycles in the desired temperature range. A decrease in the long-wavelength range was observed for the polished sample, which remained stable after the first cycle. This change is attributed to the relaxation of surface tensions produced upon polishing [27]. Due to the reproducibility of these results, they are considered to be representative of the intrinsic emissivity of Eurofer 97 in this temperature range.

A comparison of the data from Figs. 3a and 3b at two temperatures is shown in Fig. 4, together with room-temperature literature data on Grade 91 steel samples with similar surface states and root-mean-square R_q roughness values [15]. To our knowledge, there are no emissivity measurements on Eurofer 97 available in the literature to compare with. The closest material for which data could be found was a ferritic Grade 91 steel (9% Cr + 1% Mo) [12–15]. Despite non-negligible differences in composition and microstructure, the two materials are similar enough to be compared in some references for other thermophysical properties [3]. It can be appreciated that the surface state is responsible for the strongest differences in emissivity values, compared to the effects of wavelength and temperature. In both cases, the rough samples correspond to treatments which strongly deform the surface structure and create deep valleys in the ma-

terial (hot rolling in the case of Eurofer 97, and shot peening in the case of Ref. [15]). Thus, their emissivities will depend significantly on the geometrical arrangement of surface elements, especially in the presence of multiple roughness length scales, such as micro- and macro-roughness [28]. The emissivity can increase even further if the surface chemical composition is modified by processing methods such as electrical discharge machining, which also increase the variability in results [13]. Overall, finding reliable emissivity data for metallic materials is a generally difficult task. Nevertheless, this comparison shows that, as discussed in Ref. [15], the surface roughness values required to induce great emissivity changes stray far from the reasonable range generally expected for critical nuclear reactor components.

With regards to the heat-transfer capabilities of these alloys, it is important to study the angular dependence of their emissive properties in order to accurately determine its total hemispherical emissivity. Thus, for each temperature, directional measurements from 10° to 80° have been performed for both surface states. The results are shown in Fig. 5. To a first approximation, both spectra show similar tendencies, with the long-wavelength emissivities increasing to a greater extent with angle that the short-wavelength region, which remains mostly constant up to the highest angles, where it starts to drop. This is a behavior typically observed for metallic materials [21]. However, the increase with angle is much more pronounced for the polished sample, which is expected from electromagnetic theory for materials with very low emissivities.

Numerically integrated values for the total emissivities for both surface states are shown in Figs. 6a and 6b. The only total data that could be found in the literature for Grade 91 steels is shown, with total hemispherical data for a rough sample from Ref. [12] and total normal data for a polished sample from Ref. [15]. In order to better compare the results in this work to the latter, the total normal emissivity of the polished sample is also included in Fig. 6. As can be seen, a moderate agreement is observed for the data corresponding to the polished state, but a wide discrepancy is manifest for rougher surfaces. In the case of the data from Ref. [12], the values corresponding to the mildly abraded sample have been selected, as any other of the reported surface treatments increased the emissivity of the alloy even more. Interestingly, the average surface roughnesses reported

for sandblasted samples in Ref. [12] are lower than those for the as-rolled Eurofer 97 sample, while the opposite is true for the emissivity values. This reveals that the simple picture of increased emissivity with increased average roughness is incomplete, and both height and length components of roughness contribute to the thermal radiative properties [28]. The results are consistent with the relatively large value of the RSm parameter (Table 1), which characterizes the horizontal spread of the profile, whereas the profile measured in Ref. [12] features very sharp roughness features. Also, it must be noted that some aggressive roughening treatments can even modify the composition of the alloy near the surface or plastically deform the crystal bonds of the surface material. Finally, it should be mentioned that thermal simulations have cited a value of 0.25 at 573 K [4–6], which, as evident from Fig. 6, is a very high value for a polished metallic material in these temperature and wavelength ranges, and is even higher than the value for the rough as-rolled profile. It is assumed that this quoted value corresponds to the total hemispherical emissivity and has been measured using calorimetric methods, although no additional characterization is provided in the references.

In order to verify the feasibility of these measurements and the applicability of predictive models, the data corresponding to the polished surface state are compared to theoretical relations. One of the most convenients methods of estimating the emissivities of metallic materials relies on the Hagen-Rubens approximation and its extensions [19]. This approximation assumes that the relaxation time of conduction electrons is sufficiently short that their collisions become the main mechanism for absorption and emission of infrared energy. Whereas this approach is known to be in great error for many pure metals, it is expected to be valid for alloys, for which the relaxation time is very short. One of these relations (the Davisson-Weeks expression, as modified by Parker and Abbott) has been found to be in agreement with the average total hemispherical data of V-4Cr-4Ti alloys [21]:

$$\varepsilon_H = 0.766(\rho T)^{1/2} - [0.309 - 0.0889\ln(\rho T)]\rho T - 0.0175(\rho T)^{3/2} \qquad (3)$$

Comparisons of the data for the polished sample and theoretical predictions are shown in Fig. 7. Electrical resistivity data for Eurofer 97 and Grade 91 steel

have been extracted from Ref. [3], while data for F82H steel was taken from [29]. The authors of the former noted that the electrical resistivity of this material differs significantly from that of Grade 91 steel, despite their similar compositions, and suggested that differences in their magnetic properties (e.g., their Curie temperature) may account for this effect [3]. Thus, it was expected that this discrepancy will translate also into different emissivity values. However, a relative agreement between all values can be observed, which is attributed to the small sensitivity of Eq. 3 to changes in the electrical resistivity of a few percent. Moreover, the strong dependence of emissivity on surface state could obscure this comparison in real applications, although, as noted above, the roughness range for components of nuclear fusion vessels is likely much lower than the limit beyond which the surface properties significantly alter the emissivity of the piece.

As a final note, it is important to reflect on the significance of the obtained results. As discussed above, the obtained emissivity values for the polished sample are much lower than the assumed value of 0.25 reported in the literature and very similar to the predicted values for other compositions, but it is clear that the influence of extrinsic factors can mask these influences by inducing much larger effects. It is well known that both surface modifications and thermal degradation of the microstructure can increase the emissivities of materials [12, 21]. Thus, further work needs to be done to characterize nuclear alloys and the susceptibility of their emissivities to extrinsic factors, such as different surface and heat treatments, as well as radiation damage.

4. Conclusions

The infrared emissivities of as-rolled and polished Eurofer 97 follow similar trends as found in the scarce information available on similar steels in the literature for Grade 91 steels. Despite the crucial role played by surface state and roughness in modifying emissivity values, data in a polished state are consistent with literature data and can be reproduced from theoretical relations based on electrical resistivity measurements. It has also been shown that the important differences in electrical resistivity between the similar Eurofer 97, F82H, and Grade 91 steels do not manifest in strongly discrepant thermal ra-

diative properties. Finally, we can also infer that the usually quoted values for the emissivity of this material are higher than its experimental intrinsic value. Thus, some form of radiative cooling enhancement must take place for this alloy.

Acknowledgements

I. González de Arrieta thanks the Basque Government for their PhD and post-doctoral grants (PRE-2019-2-0191, POS-2020-1-0045).

References

[1] H. Tanigawa, E. Gaganidze, T. Hirose, M. Ando, S. Zinkle, R. Lindau, E. Diegele, Development of benchmark reduced activation ferritic/martensitic steels for fusion energy applications, Nuclear Fusion 57 (2017) 092004.

[2] R. Lindau, A. Möslang, M. Rieth, M. Klimiankou, E. Materna-Morris, A. Alamo, A.-A. Tavassoli, C. Cayron, A.-M. Lancha, P. Fernandez, et al., Present development status of EUROFER and ODS-EUROFER for application in blanket concepts, Fusion Engineering and Design 75 (2005) 989–996.

[3] K. Mergia, N. Boukos, Structural, thermal, electrical and magnetic properties of Eurofer 97 steel, Journal of Nuclear Materials 373 (2008) 1–8.

[4] B. Končar, M. Draksler, O. C. Garrido, B. Meszaros, Thermal radiation analysis of DEMO tokamak, Fusion Engineering and Design 124 (2017) 567–571.

[5] B. Končar, O. C. Garrido, M. Draksler, R. Brown, M. Coleman, Initial optimization of DEMO fusion reactor thermal shields by thermal analysis of its integrated systems, Fusion Engineering and Design 125 (2017) 38–49.

[6] O. C. Garrido, B. Končar, S. Košmrlj, C. Bachmann, B. Meszaros, Global thermal analysis of DEMO tokamak, in: 24th International Conference Nuclear Energy for New Europe, 2014, pp. 14–17.

[7] Y. Igitkhanov, R. Fetzer, L. Boccaccini, B. Bazylev, Thermo-mechanical analysis of the DEMO FW module, Physica Scripta 90 (2015) 105601.

[8] I. García-Cortés, E. Abad, R. Martínez-Ballarín, J. Bermejo, A. Ibarra, R. Vila, Preliminary design study of a proton irradiation laboratory for fusion materials at ESS-Bilbao, Fusion Engineering and Design 87 (2012) 1839–1845.

[9] S. Gordeev, F. Schwab, F. Arbeiter, Y. Qiu, Numerical study of conjugated heat transfer for DONES high flux test module, Fusion Engineering and Design 146 (2019) 609–613.

[10] D. Bernardi, P. Arena, G. Bongiovì, P. Di Maio, M. Frisoni, G. Miccichè, M. Serra, Analysis of the thermomechanical behavior of the IFMIF bayonet target assembly under design loading scenarios, Fusion Engineering and Design 96 (2015) 217–221.

[11] M. Ida, T. Chida, K. Furuya, E. Wakai, H. Nakamura, M. Sugimoto, Thermal-stress analysis of IFMIF target back-wall made of reduced-activation ferritic steel and austenitic stainless steel, Journal of nuclear materials 386 (2009) 987–990.

[12] C. B. Azmeh, K. L. Walton, T. K. Ghosh, S. K. Loyalka, D. S. Viswanath, R. V. Tompson, Total hemispherical emissivity of grade 91 ferritic alloy with various surface conditions, Nuclear Technology 195 (2016) 87–97.

[13] F. N. Al Zubaidi, K. L. Walton, R. V. Tompson, T. K. Ghosh, S. K. Loyalka, Emissivity of Grade 91 ferritic steel: Additional measurements on role of surface conditions and oxidation, Nuclear Technology (2020) 1–13.

[14] G. Cao, S. Weber, S. Martin, M. Anderson, K. Sridharan, T. Allen, Spectral emissivity measurements of candidate materials for very high temperature reactors, Nuclear Engineering and Design 251 (2012) 78–83.

[15] J. King, H. Jo, R. Tirawat, K. Blomstrand, K. Sridharan, Effects of surface roughness, oxidation, and temperature on the emissivity of reactor pressure vessel alloys, Nuclear Technology 200 (2017) 1–14.

[16] S. I. Woods, T. M. Jung, D. R. Sears, J. Yu, Emissivity of silver and stainless steel from 80 K to 300 K: application to ITER thermal shields, Cryogenics 60 (2014) 44–48.

[17] T. S. Hunnewell, K. L. Walton, S. Sharma, T. K. Ghosh, R. V. Tompson, D. S. Viswanath, S. K. Loyalka, Total hemispherical emissivity of SS 316L with simulated very high temperature reactor surface conditions, Nuclear Technology 198 (2017) 293–305.

[18] J. L. King, H. Jo, A. Shahsafi, K. Blomstrand, K. Sridharan, M. A. Kats, Impact of corrosion on the emissivity of advanced reactor structural alloys, Journal of Nuclear Materials 508 (2018) 465–471.

[19] A. Sievers, Thermal radiation from metal surfaces, Journal of the Optical Society of America 68 (1978) 1505–1516.

[20] M. Balden, S. Elgeti, M. Zibrov, K. Bystrov, T. Morgan, Effect of the surface temperature on surface morphology, deuterium retention and erosion of EUROFER steel exposed to low-energy, high-flux deuterium plasma, Nuclear Materials and Energy 12 (2017) 289–296.

[21] T. Echániz, I. G. de Arrieta, R. Fuente, I. Urcelay-Olabarria, J. Igartua, N. de la Pinta, W. Ran, H. Fu, J. Chen, P. F. Zheng, M. J. Tello, G. A. López, Thermal radiative properties of electron-beam-melted and mechanically alloyed V-4Cr-4Ti based alloys between 200 and 750 °C, Journal of Nuclear Materials 513 (2019) 86–93.

[22] J. Hoffmann, M. Rieth, L. Commin, P. Fernández, M. Roldán, Improvement of reduced activation 9% Cr steels by ausforming, Nuclear Materials and Energy 6 (2016) 12–17.

[23] I. González de Arrieta, T. Echániz, R. Fuente, J. M. Campillo-Robles, J. M. Igartua, G. A. López, Updated measurement method and uncertainty budget for direct emissivity measurements at the University of the Basque Country, Metrologia 57 (2020) 045002.

[24] Joint Committee for Guides in Metrology, Evaluation of measurement data - Supplement 1 to the "Guide to the expression of uncertainty in measure-

ment" - Propagation of distributions using a Monte Carlo method, Technical Report JCGM 101:2008, 2008.

[25] M. Klimenkov, R. Lindau, E. Materna-Morris, A. Möslang, TEM characterization of precipitates in EUROFER 97, Progress in Nuclear Energy 57 (2012) 8–13.

[26] V. B. Oliveira, K. D. Zilnyk, H. R. Z. Sandim, Thermodynamic simulation of reduced activation ferritic–martensitic Eurofer-97 steel, Journal of Phase Equilibria and Diffusion 38 (2017) 208–216.

[27] L. González-Fernández, E. Risueño, R. Pérez-Sáez, M. Tello, Infrared normal spectral emissivity of Ti–6Al–4V alloy in the 500–1150 K temperature range, Journal of Alloys and Compounds 541 (2012) 144–149.

[28] Y. Yang, R. O. Buckius, Surface length scale contributions to the directional and hemispherical emissivity and reflectivity, Journal of Thermophysics and Heat Transfer 9 (1995) 653–659.

[29] T. Hirose, T. Nozawa, R. E. Stoller, D. Hamaguchi, H. Sakasegawa, H. Tanigawa, H. Tanigawa, M. Enoeda, Y. Katoh, L. L. Snead, Physical properties of F82H for fusion blanket design, Fusion Engineering and Design 89 (2014) 1595–1599.

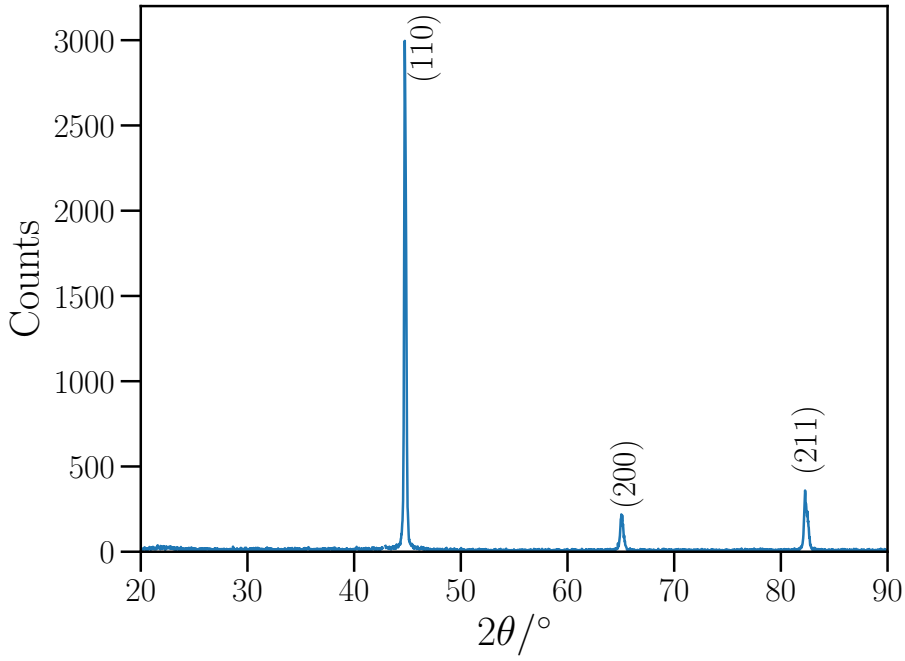

Figure 1: X-ray diffractogram (Cu K_α) of Eurofer 97. The observed peaks have been indexed to a BCC structure.

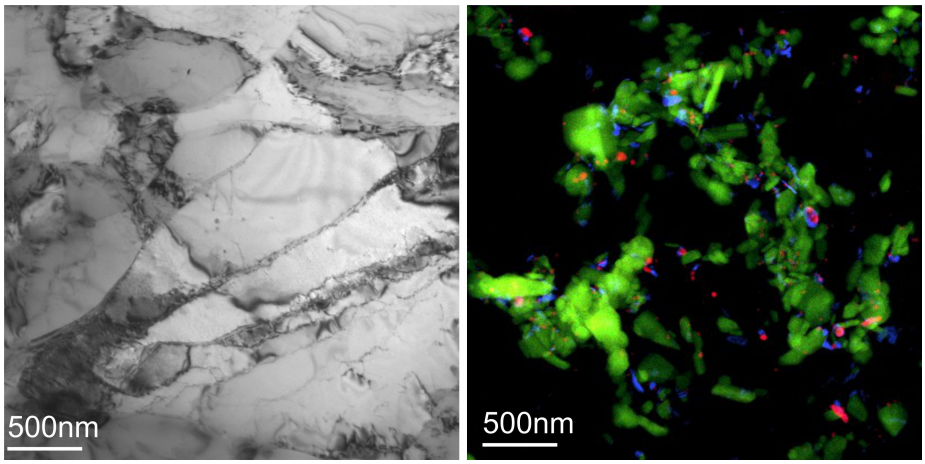

Figure 2: (a) Low-magnification bright-field TEM micrograph of Eurofer 97. (b) Distribution of secondary phases: $M_{23}C_6$ (green), VN (blue), and TaC (red).

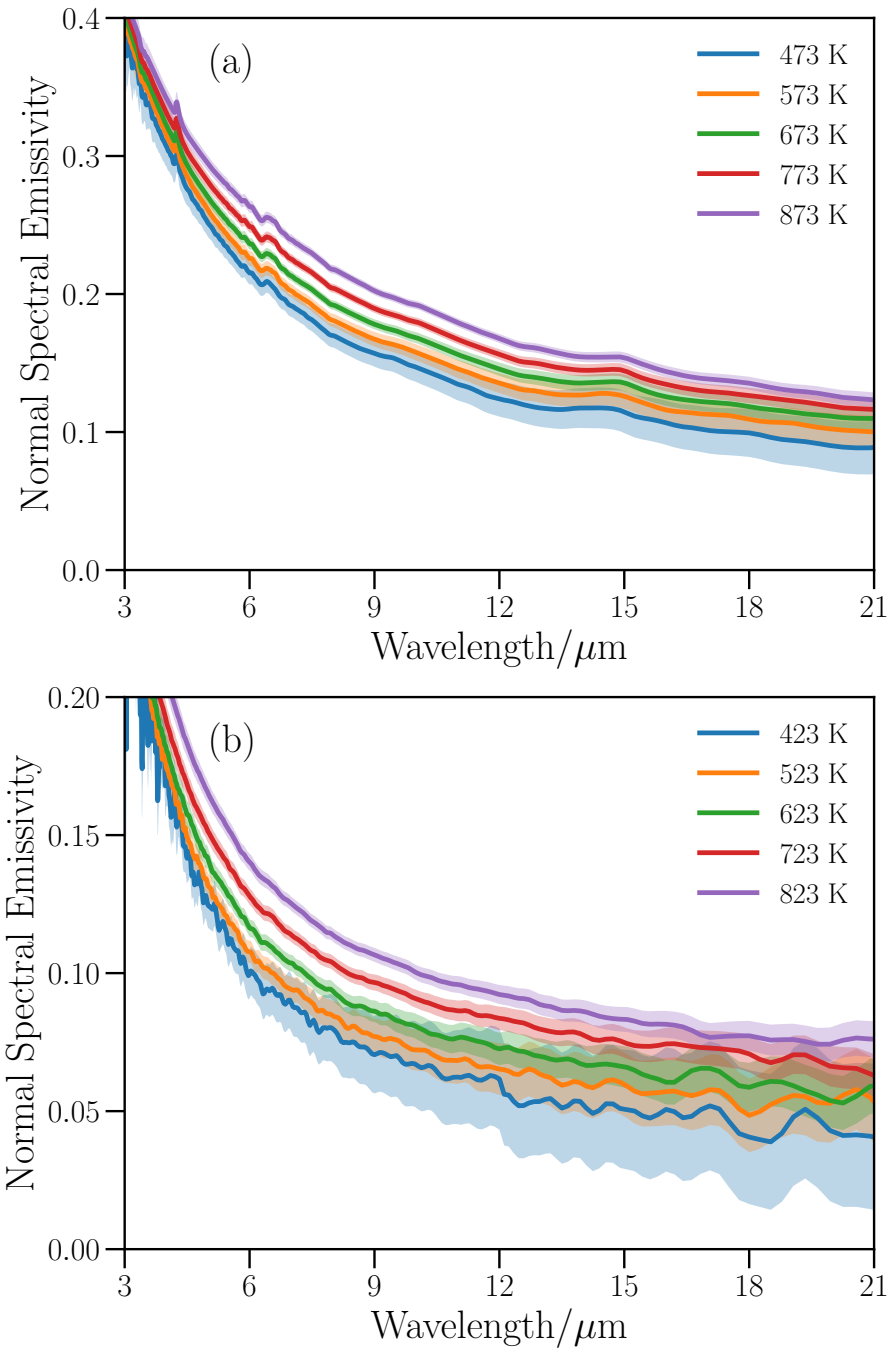

Figure 3: Normal spectral emissivity of Eurofer 97 in (a) as-rolled and (b) polished states. Shaded areas correspond to expanded uncertainties (coverage factor $k = 2$).

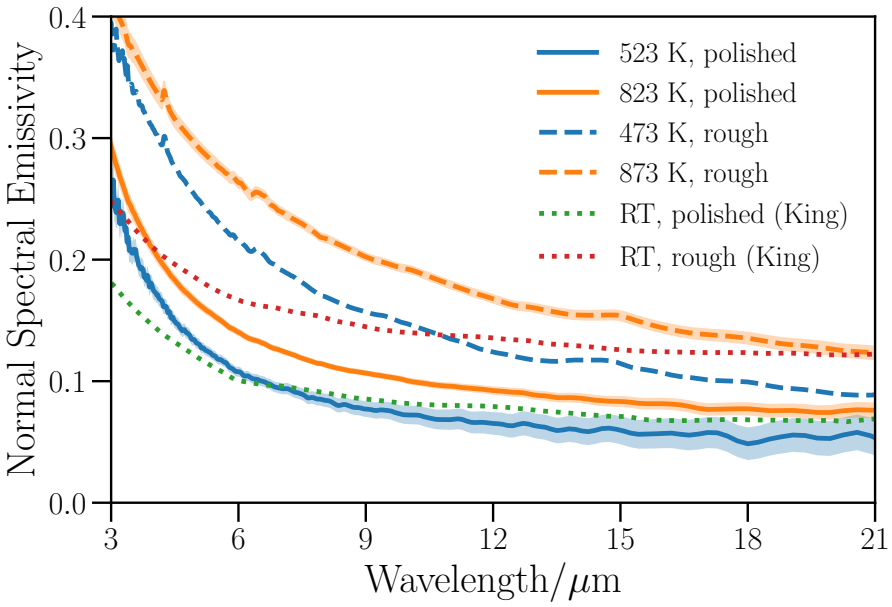

Figure 4: Normal spectral emissivities of as-rolled and polished Eurofer 97 at two temperatures, compared to room-temperature literature data for 91 steel for two surface states [15]. Shaded areas correspond to expanded uncertainties (coverage factor $k = 2$).

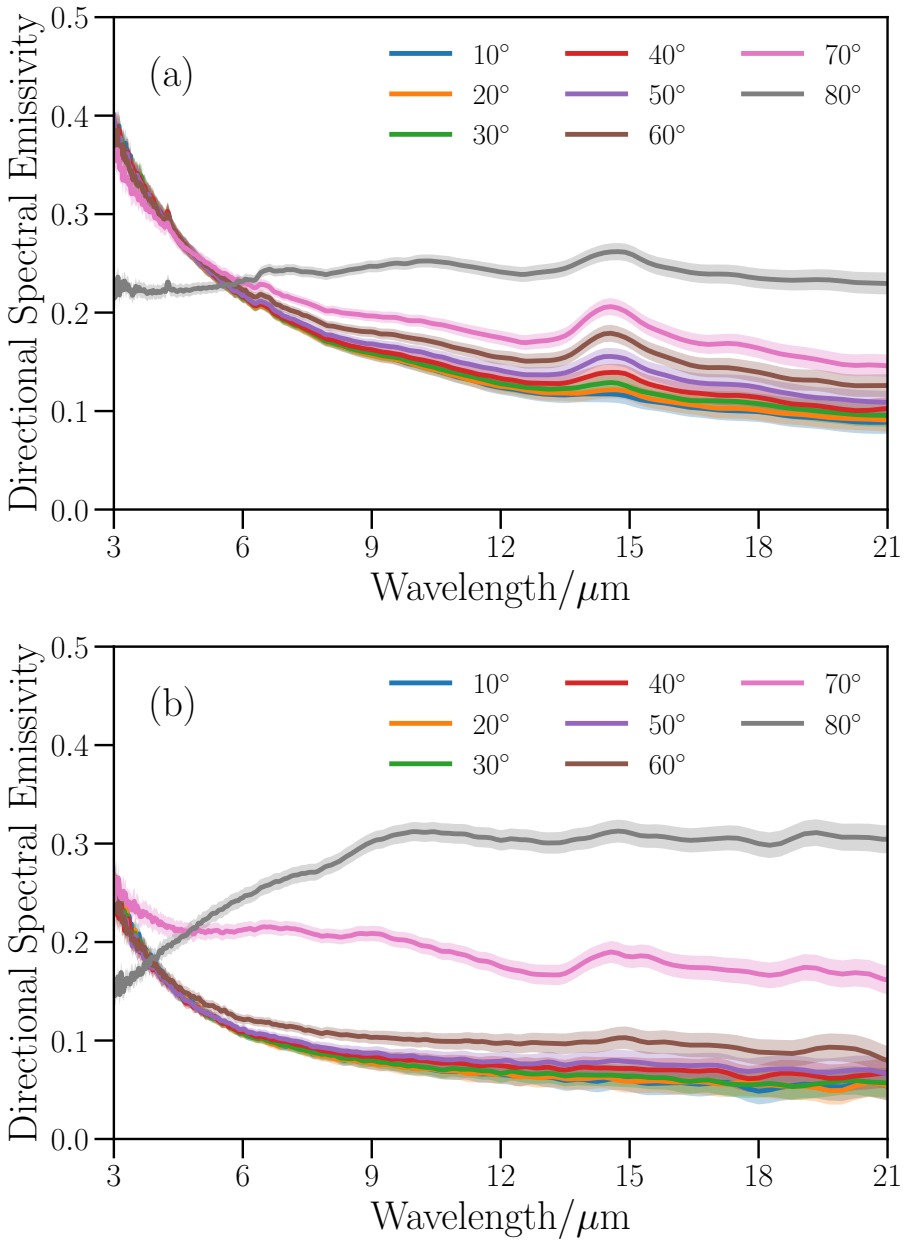

Figure 5: Directional spectral emissivities of (a) as-rolled and (b) polished Eurofer 97 at 573 and 523 K, respectively. Shaded areas correspond to expanded uncertainties (coverage factor $k = 2$).

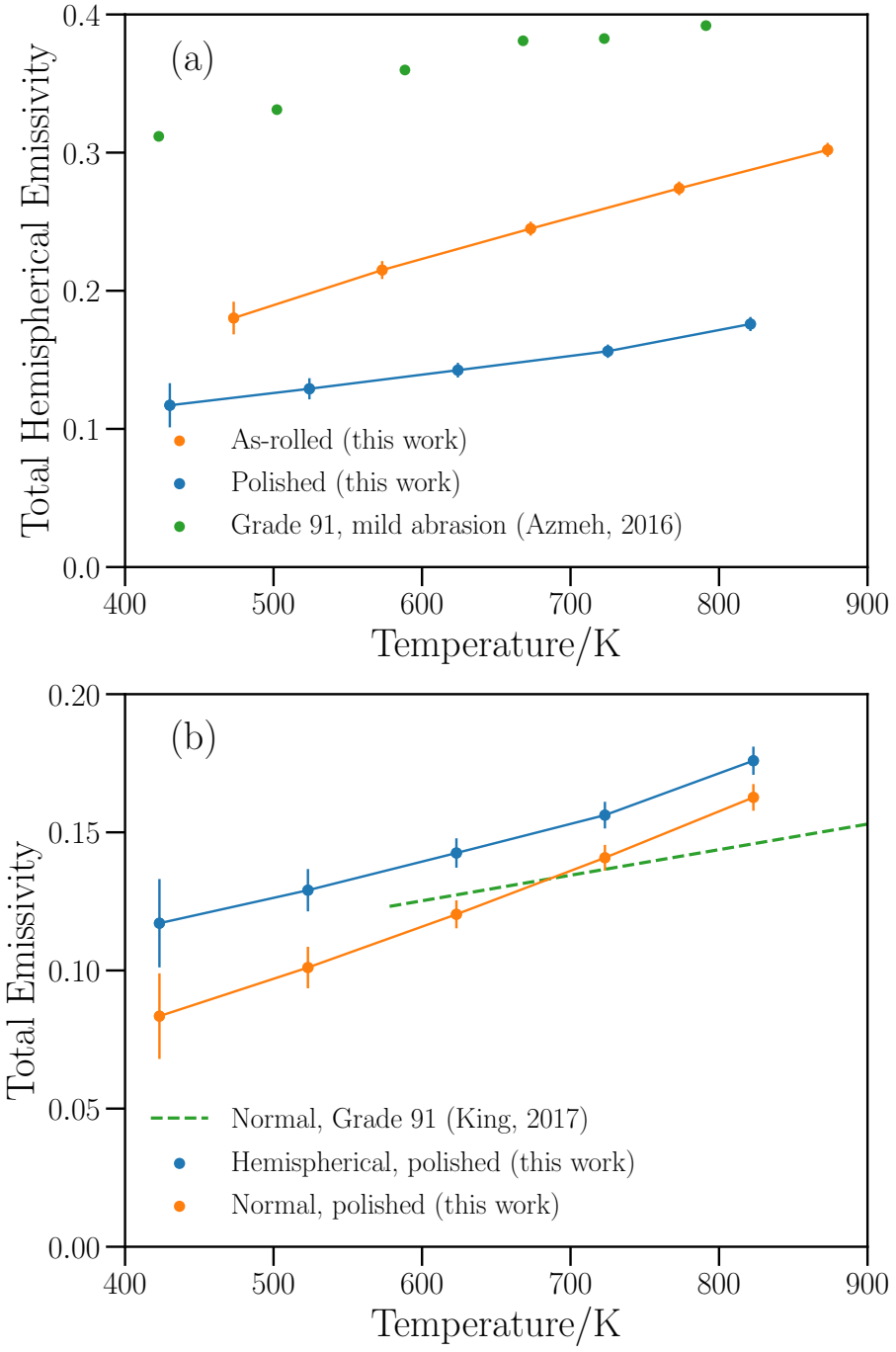

Figure 6: Total hemispherical emissivities of as-rolled and polished Eurofer 97, compared to literature data on 91 steel [12, 15]. Error bars correspond to expanded uncertainties (coverage factor $k = 2$).

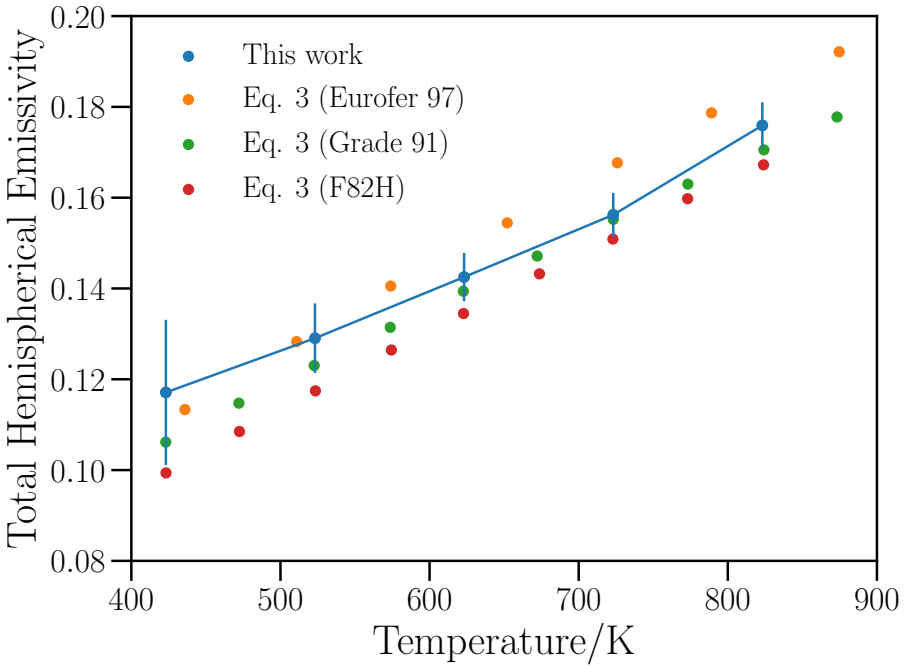

Figure 7: Total hemispherical emissivity of polished Eurofer 97, compared to the values predicted by Eq. 3 using electrical resistivity data from Ref. [3] (Eurofer 97 and Grade 91) and Ref. [29] (F82H). Error bars correspond to expanded uncertainties (coverage factor $k = 2$).